



Published in final edited form as:

Nat Methods. 2019 May ; 16(5): 417–420. doi:10.1038/s41592-019-0391-1.

A photo-cleavable surfactant for top-down proteomics

Kyle A. Brown¹, Bifan Chen¹, Tania M. Guardado-Alvarez¹, Ziqing Lin^{2,3}, Leekyoung Hwang¹, Serife Ayaz-Guner², Song Jin¹, and Ying Ge^{*,1,2,3}

¹Department of Chemistry, University of Wisconsin–Madison, Wisconsin 53719, USA.

²Department of Cell and Regenerative Biology, University of Wisconsin–Madison, Wisconsin 53719, USA.

³Human Proteomics Program, School of Medicine and Public Health, University of Wisconsin–Madison, Wisconsin 53719, USA.

Abstract

We report the identification of a photo-cleavable anionic surfactant, 4-hexylphenylazosulfonate (Azo) that can be rapidly degraded upon UV irradiation, for top-down proteomics. Azo can effectively solubilize proteins with performance comparable to SDS and is mass spectrometry (MS)-compatible. Importantly, Azo-aided top-down proteomics enables the solubilization of membrane proteins for comprehensive characterization of post-translational modifications. Moreover, Azo is simple to synthesize and can be used as a general SDS replacement in SDS-PAGE.

A comprehensive analysis of “proteoforms” that arise from genetic variations and post-translational modifications (PTMs) is essential for deciphering biological systems at a functional level¹. The conventional “bottom-up” proteomics analyzes peptides from protein digests which does not directly identify proteoforms and is suboptimal for characterizing PTMs and sequence variants¹. In contrast, top-down mass spectrometry (MS)-based proteomics analyzes intact proteins and is the most powerful method to comprehensively characterize proteoforms deciphering the PTMs together with sequence variations^{1–3}. However, despite significant promises, top-down proteomics still faces major challenges⁴.

Users may view, print, copy, and download text and data-mine the content in such documents, for the purposes of academic research, subject always to the full Conditions of use:http://www.nature.com/authors/editorial_policies/license.html#terms

*Correspondence should be addressed to Y.G. (ying.ge@wisc.edu).

Author contributions

K.B. designed and performed experiments, analyzed the data, and wrote the manuscript. B.C. designed and performed experiments, analyzed the data, and wrote the manuscript. T.G. designed and performed experiments, analyzed the data, and wrote the manuscript. Z. L. performed experiments and analyzed the data. L.H. performed experiments and analyzed the data. S. A-G. performed experiments and analyzed the data. S.J. designed the experiments, supervised the project, and wrote the manuscript. Y.G. conceived the idea, designed the experiments, supervised the project, and wrote the manuscript.

Online content

Methods, Supplementary Notes, Tables, and Figures, Nature Life Science Reporting Summary, source data files, and statements of data availability are available at (DOI).

Additional information

Supplementary information is available for this paper at (doi).

Competing interests

The University of Wisconsin-Madison has filed a provisional patent application P180335US01; US serial no. 62/682027 (June 7, 2018) on the basis of this work. Y.G., S.J., K.B., and T.G. are named as inventors on the provisional patent application.

One such challenge in top-down proteomics is protein solubility⁴, especially for membrane proteins, which comprise a large proportion of the proteome and play a critical role in many cellular functions and are important drug targets^{5,6}. To effectively extract proteins from cells or tissues, surfactants (also known as detergents) are commonly included in the extraction buffer⁶. Unfortunately, conventional ionic surfactants are not compatible with MS because they greatly suppress protein MS signal^{6,7}. Therefore, surfactants need to be removed prior to MS analysis, which may result in protein loss and degradation^{8,9}. Developing MS-compatible surfactants that can be quickly degraded into innocuous non-surfactant byproducts prior to MS analysis can help address the protein solubility challenge in top-down proteomics. Efforts have been made in developing various acid-labile surfactants which have been effective for bottom-up proteomics^{10–13}, however none have demonstrated direct compatibility with intact protein MS for top-down proteomics.

Distinct from the previous approaches using acid-labile surfactants^{10–13}, herein we design and develop photo-cleavable surfactants by inserting a photo-cleavable moiety in between the hydrophilic head and hydrophobic tail that can be rapidly cleaved and degraded upon UV irradiation prior to MS analysis (Fig. 1a). Degradation via a photochemical reaction has the advantages of being simple, fast, and can be easily controlled by turning a UV lamp on and off^{14–16}. Our goal is to identify a strong photo-cleavable surfactant that can effectively solubilize proteins during sample preparation with similar performance to sodium dodecyl sulfate (SDS)⁸, but is compatible with top-down proteomics.

We performed a systematic screening of many synthesized candidates (Supplementary Note 1–3 and Supplementary Table 1) and identified 4-hexylphenylazosulfonate¹⁷ (Fig. 1b and Supplementary Fig. 1–2), hereafter referred to as “Azo”, to be the top-performing surfactant, as it not only is water-soluble, but also greatly improves protein extraction (Supplementary Table 1). Notably, Azo was simple to synthesize, requiring only two steps (Fig. 1c), and could be effectively purified by recrystallization, making it an ideal candidate for general use as a surfactant in biochemical applications. For instance, we have used Azo instead of SDS to perform polyacrylamide gel electrophoresis (PAGE) (Supplementary Fig. 3), demonstrating that Azo could be used as a SDS replacement in SDS-PAGE.

We further investigated the photo-degradation kinetics of the Azo dissociating into 4-hexylphenol, 4-hexylbenzene, nitrogen, and hydrogen sulfate¹⁴ (Fig 1b) upon irradiation with a 100 W high pressure mercury lamp for 0, 10, 30, 60, 90, and 120 s using UV-Vis spectroscopy (Fig. 1d). By comparing several degradation conditions, we found that the presence of organic solvent and acid facilitates rapid degradation of Azo (Supplementary Fig. 4).

Next, we examined the efficacy of Azo for solubilizing proteins from cardiac tissues using a direct side-by-side comparison with SDS, and its acid-labile mimic, MS-compatible slowly degradable surfactant (MaSDeS)¹⁰, as well as dodecyl β -D-maltoside (DDM), a commonly used surfactant for native MS¹⁸. The SDS-PAGE gel (Fig. 1e) and protein assay (Fig. 1f) show that the addition of 0.5% Azo to the extraction buffer, labelled as E3(Azo), drastically improved the solubilization of proteins when compared to the control without surfactant, E3(NS), which barely solubilized proteins after the depletion of soluble proteins using

HEPES buffer, E1 and E2. Overall, the anionic surfactants, Azo, SDS, and MaSDeS, are highly effective in solubilizing proteins compared to the non-ionic surfactant, DDM (Fig. 1e,f). Furthermore, a Western blot analysis confirmed the presence of common cardiac membrane proteins in E3(Azo), demonstrating the successful extraction of integral membrane proteins by Azo (Supplementary Fig. 5).

More importantly, Azo surfactant is MS-compatible. We first performed direct infusion ESI-MS analysis using ubiquitin (Ubi) in the presence of 0.1% of a chosen surfactant, without an additional desalting step (Fig. 1g). The results showed the presence of 0.1% SDS completely suppressed the MS signal and 0.1% MaSDeS significantly suppressed the MS signal. In contrast, 0.1% DDM and 0.1% Azo yielded comparable MS signals, showing minimal signal suppression when compared to the control with no surfactant (Fig. 1g). We also examined the effect of the UV-irradiation on MS analysis of proteins and found that Azo had minimal effect on the qualitative and quantitative analysis of intact proteins in the presence of reducing agent, tris(2-carboxyethyl)phosphine hydrochloride (TCEP), or free methionine (Supplementary Note 4, Supplementary Fig. 6–9). Furthermore, we have performed a systematic comparison of Azo with a broader range of commonly used surfactants to evaluate their ability to solubilize proteins from the insoluble cardiac tissue pellets and subsequently assessed their MS-compatibility (Supplementary Note 5 and Supplementary Fig. 10–12). We concluded that among all the surfactants evaluated, Azo is the only surfactant that not only can effectively solubilize proteins but also is compatible with top-down MS analysis of intact proteins.

Next, we assessed the utility of Azo for top-down proteomics in online reversed-phase chromatography (RPLC)-MS and RPLC-MS/MS experiments (Supplementary Table 2) with collision-induced dissociation (CID). Water-insoluble cardiac tissue pellets were extracted with 25 mM NH_4HCO_3 buffer either containing 0.5% Azo [E3(Azo)] or no surfactant [E3(NS)] (Supplementary Fig. 13a). Notably, both the SDS-PAGE gel (Fig. 1e) and the total ion current (Supplementary Fig. 13b) showed significant increases in protein concentration and MS signal, respectively, with the use of Azo when compared to no surfactant. In a *single* RPLC/MS run, we observed 663 *unique* proteoforms in E3(Azo), in contrast to E3(NS) where only 6 unique proteoforms were detected (Supplementary Fig. 13c,d and Supplementary Table 4). Moreover, we have detected a total of 2836 proteoforms based on accurate mass measurements (Supplementary Table 3) from the combination of three LC-MS runs; among which 388 proteoforms were identified based on one-dimensional online RPLC-MS/MS data (Supplementary Table 4) representing 171 proteins (Supplementary Table 5) from mitochondria, nucleus, plasma membrane, cytoskeleton, endoplasmic reticulum, cytoplasm, and extracellular region (Supplementary Fig. 13e,f and Supplementary Note 6).

Importantly, we have observed various PTMs included acetylation, methylation, phosphorylation, and palmitoylation (Supplementary Table 5–10). In addition to the breadth in increased protein identifications, Azo also greatly improved the depth of the detection and revealed many proteins that were undetectable in the control sample (Supplementary Fig. 14a–j). For example, for the first time, Azo enabled the detection and identification of multiple proteoforms of an important Z-disk protein, calsarcin-1 (Supplementary Fig. 14d).

Because surfactants are beneficial for solubilization of peripheral and integral membrane proteins, we further show that Azo can effectively extract and enable the top-down proteomic analysis of membrane proteins from cardiac tissues (Fig. 2 and Supplementary Fig. 15) as well as human embryonic kidney (HEK) 293T cells (Supplementary Fig. 16 and Supplementary Table 9–10). Under the optimal UV-degradation conditions (which include organic solvent at low pH), many hydrophobic proteins were soluble post Azo-degradation. Using cardiac tissue as an example, we identified several important integral membrane proteins such as phospholamban (PLN), receptor-expressing enhancing protein, and succinate dehydrogenase cytochrome b560 with 1, 2, and 3 transmembrane domains (TMD), respectively (Fig. 2a,b and Supplementary Fig. 17). Notably, we not only detected intact unmodified PLN, but also its highly abundant palmitoylated proteoform (Fig. 2a). We confidently localized the palmitoylation modification to cysteine 36 within the transmembrane region based on the unmodified b₃₃ ion and the palmitoylated b₃₈ ion (Fig. 2a and Supplementary Fig. 18). PLN is a well-known cardiac regulatory protein which has been implicated in cardiomyopathy¹⁹. Similarly, we have characterized receptor-expressing enhancing protein and localized an acetylation site to the N-terminus (Fig. 2b).

Moreover, we confidently identified 46 subunits of the electron transport chain (Supplementary Table 6) and 51 proteins with TMDs (Supplementary Table 7) directly from cardiac tissue. Notably, all the subunits of the endogenous ATP synthase complex were identified with high mass accuracy (Fig. 2c). This enzyme, which plays a critical role in biological energy metabolism²⁰, includes a domain located in the inner mitochondrial membrane (IMS) (e, f, g, ATP6, ATP8, DAPIT, c, 6.8PL) as well as a domain in the mitochondrial matrix (α, β, b, ε, δ, OCSP, F₆, d, γ). In particular, Azo facilitated the identification of ATP6 (also known as ATP synthase subunit a; M_r 24952.55) with 6 TMD as well as the localization of a trimethylation to lysine 43 between 2 TMD of ATP synthase subunit c (Supplementary Fig. 19). Besides the small and intermediate size subunits (< 30 kDa), with the use of Azo, we were able to detect and identify the high molecular weight (> 50 kDa) ATP synthase subunits: ATP synthase α and β (Fig. 2c). We observed highly efficient CID fragmentation which preferentially cleaved in the transmembrane domain portions of the proteins (Fig. 2a,b and Supplementary Fig. 17–19), leading to confident protein identification of these integral membrane proteins and localization of PTMs in online RPLC-MS/MS experiments (Supplementary Table 4–10). Thus, Azo enables the detection and comprehensive characterization of these important cardiac membrane protein complexes, which opens up new opportunities to uncover their molecular basis in health and disease.

In summary, we have developed a photo-cleavable MS-compatible surfactant to increase protein solubility and enabled a general, high-throughput method for top-down proteomics. Among all the surfactants we have evaluated, we found that 4-hexylphenylazosulfonate (Azo) to be the only strong surfactant capable of effectively solubilizing proteins, including membrane proteins, without hindering downstream top-down MS analysis. Azo has the potential to further enhance top-down global proteomics when coupled to multidimensional separation, complementary fragmentation techniques, and improved data acquisition strategies⁴ (Supplementary Note 6). We expect that Azo will facilitate a myriad of proteomic

studies for understanding disease mechanisms and clinical diagnosis. Given surfactants' instrumental roles in biochemical research, we envision this photo-cleavable surfactant will have a broader impact beyond proteomics. Notably, because Azo can be easily synthesized and purified, it can be used as a cleavable SDS-replacement in general biochemical applications, for example, in SDS-PAGE.

Online methods

Materials and reagents.

All chemicals and reagents were used as received without further purification unless otherwise noted. Sodium nitrate (NaNO_3), sodium sulfite (Na_2SO_3), 4-nitrophenyl chloroformate, sodium carbonate, 4-n-hexylaniline, 4-n-octylaniline, 4-n-decylaniline, 4-n-dodecylaniline, N-(3-Dimethylaminopropyl)-N'-ethylcarbodiimide hydrochloride (EDC), 4-(bromomethyl)-3-nitrobenzoic acid, octylamine, decylamine, dodecylamine, N-ethyl-diisopropylamine (EDIPA), piperidine, 1,4-butanediol, anhydrous N,N-dimethylformamide (DMF), N,N,N',N'-Tetramethyl-O-(1H-benzotriazol-1-yl)uronium hexafluorophosphate (HBTU), and dinitrophenylhydrazine (DNP) were obtained from TCI America (Portland, OR, USA). Fmoc-photolabile linker was purchased from Advanced Chemtech (Louisville, KY, USA). Tetrahydrofuran (THF), ammonium hydroxide (NH_4OH), hexafluoroisopropanol (HFIP), dichloromethane, heptane, acetone, trimethylamine (Et_3N), magnesium sulfate (MgSO_4), sodium carbonate and silica were purchased from Sigma-Aldrich Inc. (St. Louis, MO, USA). Extraction solutions were made in nanopure deionized (DI) water (H_2O) from Milli-Q water (Millipore, Corp., Billerica, MA, USA). HEPES, ammonium bicarbonate (NH_4HCO_3), sucrose, sodium fluoride (NaF), phenylmethanesulfonyl fluoride (PMSF), ethylenediaminetetraacetic acid (EDTA), n-dodecyl β -D-maltoside (DDM), octyl β -D-glucopyranoside (OG), sodium dodecyl sulfate (SDS), digitonin (DGT), protease inhibitor cocktail, tri(2-carboxyethyl) phosphine hydrochloride (TCEP), dithiothreitol (DTT), 2-mercaptoethanol (2-ME), β -casein from bovine milk, ubiquitin from bovine erythrocytes (Ubi), bovine serum albumin (BSA), myoglobin from equine heart (Myo) and cytochrome c (Cyt c) from equine heart, ribonuclease A (RNase A) and ribonuclease B (RNaseB) from bovine pancreas were purchased from Sigma-Aldrich Inc. (St. Louis, MO, USA). ProteaseMaxTM (PM)²¹ was obtained from Promega (Fitchburg, WI, USA). RapiGestTM (RG also known as ALS)^{11, 13} was purchased from Waters (Milford, MA, USA). Sodium orthovanadate, HPLC grade H_2O , acetonitrile (ACN), methanol (MeOH), ethanol (EtOH), optima LC-MS grade formic acid, optima LC-MS grade isopropanol (IPA), Pierce protein-free tris-buffered saline (TBS) blocking buffer, tween 20, and molecular weight cutoff (10 and 30 kDa MWCO) (0.5 mL) centrifugal filters, Coomassie blue R-250, and Dulbecco's modified eagle medium (DMEM) were purchased from Fisher Scientific (Waltham, MA). Goat Anti-Antigen: Rabbit IgG (H +L), Goat Anti-Antigen: mouse IgG (H+L), BCA protein assay, and Pierce 660 nm Protein Assay Reagent, Ionic Detergent Compatibility Reagent were purchased from Thermo Fisher (Waltham, MA). Protein Assay Dye Reagent Concentrate was purchased from BioRad (Hercules, CA). Voltage-dependent anion-selective channel (VDAC) antibody was purchased from Biovision (Milpitas, CA). Mitochondrial import receptor subunit (TOM20) was purchased from Santa Cruz Biotechnology (Dallas, Tx). Sodium potassium adenosine

triphosphate (Na-K ATPase) and cadherin antibodies were purchased from Abcam (Cambridge, United Kingdoms). Phospholamban antibody was purchased from Bioss (Woburn, MA). Fetal bovine serum (FBS) was purchased from Life Technologies (Carlsbad, CA). Mini-gels (12.5%) for SDS polyacrylamide gel electrophoresis (SDS-PAGE) were prepared in house using acrylamide/Bis-Acryamide (37.5:1) 40% solution purchased from Hoefer (Holliston, MA). MS-compatible degradable surfactant (MaSDeS) was synthesized by Promega and provided to us as a gift as described previously¹⁰.

Synthesis of O-nitrobenzyl (ONB) surfactant family.

Synthesis of 4-(hydroxyethyl)-3-nitrobenzoic acid.—A solution of 500 mg of 4-(bromomethyl)-3-nitrobenzoic acid (1.92 mmol) and 814 mg of Na₂CO₃ (7.68 mmol) in 16 mL of a mixture of H₂O/acetone 1:1 (v/v) was refluxed for 5 h. The acetone was then evaporated and the resulting solution was washed with 9 mL of diethyl ether. After the wash, the solution was acidified with 18% hydrochloric acid until a precipitate was observed. The product was then extracted with ethyl acetate (3 × 12 mL). The concentrated organic layer was washed with H₂O (6 mL) and dried over MgSO₄. The dry organic layer was filtered and concentrated *in vacuo* to yield 74% of 4-(hydroxyethyl)-3-nitrobenzoic acid as a yellow solid²².

Synthesis of intermediate product I (C12) (Supplementary Note 1).—Using a traditional EDC coupling, 270 mg of 4-(hydroxyethyl)-3-nitrobenzoic acid (1.37 mmol) was reacted with 0.32 mL of dodecylamine (1.37 mmol) to produce **1** (n= 10, C12) in a 44% yield.

Synthesis of intermediate product I (C8) (Supplementary Note 1).—Using a traditional EDC coupling, 300 mg of 4-(hydroxyethyl)-3-nitrobenzoic acid (1.52 mmol) was reacted with 0.25 mL of octylamine (1.37 mmol) to produce **1** (n= 6, C8) in a 19% yield.

Synthesis of intermediate product I (C6) (Supplementary Note 1).—Using a traditional EDC coupling, 300 mg of 4-(hydroxyethyl)-3-nitrobenzoic acid (1.52 mmol) was reacted with 0.20 mL of hexylamine (1.37 mmol) to produce **1** (n= 4, C6) in a 46% yield.

Synthesis of intermediate product IIs (Supplementary Note 1).—7.7 mmol of each intermediate product I was dissolved in 40 mL of THF and the solution was cooled to 0 °C. While stirring, 4-nitrophenylchloroformate was slowly added to the THF solution. Then 0.16 mL of pyridine was added dropwise over 20 min and the reaction was stirred for an additional 2 h. The reaction was then filtered. The final product was purified using a silica column that was packed using a solvent of 7:3 ratio of heptane: EtOH and an eluting solvent of a ratio of 4:1 heptane: EtOH²³.

Synthesis of ONB final product (Supplementary Note 1).—0.13 mmol of intermediate product II was dissolved in 2.3 mL of THF. In a separate container, 0.2 mmol of 3-aminopropane sulfonic acid sodium salt in 0.43 mL of water was added to the THF solution. The reaction was stirred overnight at 50 °C. The product was purified using a silica column with a mixture of dichloromethane:MeOH (1:5). The final product was confirmed by

electrospray ionization mass spectrometry (ESI-MS). ESI mass spectra for the synthesized ligand molecules were obtained using a Waters (Micromass) LCT[®] mass spectrometer. ONB **C12** (C₂₄H₃₈N₃O₈SNa), [M-Na+H+NH₄]⁺: calculated *m/z*: 547.6, observed *m/z*: 547.3; ONB **C8** (C₂₀H₃₀N₃O₈SNa), [M-Na+H+NH₄]⁺: calculated *m/z*: 491.5, observed *m/z*: 491.3; ONB **C6** (C₁₈H₂₆N₃O₈SNa), [M-Na+H+NH₄]⁺: calculated *m/z*: 463.5, observed *m/z*: 463.3.

Synthesis of O-nitroveratryl (ONV) surfactant family.

The ONV surfactants were synthesized following previously reported procedures¹⁵. Briefly, to a solution of Fmoc-ONV-COOH (0.57 mmol) and HBTU (0.69 mmol) in 3.5 mL of anhydrous DMF, EDIPA (1.2 mmol) was added drop wise. The solution was cooled on ice and added to a solution of dodecylamine in 0.5 mL of ice-cold EtOH. After stirring for 30 min at 0 °C, the mixture was stirred overnight at room temperature (RT). The resulting precipitate was filtered and washed with DMF followed by *in vacuo* drying. Intermediate product I (**n= 10, C12**) was obtained as an amorphous white powder. Similar procedure were followed for **n= 8, C10** and **n= 6, C8** (Supplementary Note 2).

Synthesis of NH₂-ONV-CH₂ (CH₂)_n CH₃ (Intermediate product II)

(Supplementary Note 2).—Piperidine was added dropwise to a solution of intermediate product I (0.6 mmol) in anhydrous DMF (3 mL) to reach a final concentration of 2 M. The solution was stirred at RT for 2 h, and then DMF was removed by evaporation. The residual was dissolved in MeOH and the resulting precipitate was removed by filtration. A pale yellow solid was obtained after evaporation of the filtered solution.

Synthesis of Sulfonate-ONV-CH₂ (CH₂)_n CH₃ (Final product) (Supplementary

Note 2).—1,4-butanediol (2.1 eq, 0.74 mmol) was added to a solution of intermediate product II (1.0 eq, 0.35 mmol) with Et₃N (2.0 eq) in ACN (2 mL) and then the flask was sealed. The mixture was stirred and heated to ~90 °C for 48 h. After removing the solvent by evaporation, a light yellow viscous oil was obtained quantitatively. The oil was suspended in water and a NH₄OH (aq) solution was added dropwise until pH ~8 was reached. The surfactant solutions were centrifuged. The final product was confirmed by ESI-MS. ONV **C12** (C₂₉H₅₀N₃O₈SNa), [M-Na]⁻, calculated *m/z*: 600.3, observed *m/z*: 600.3; ONV **C10** (C₂₇H₄₆N₃O₈SNa), [M-Na]⁻, calculated *m/z*: 572.3, observed *m/z*: 572.2. ONV **C8** (C₂₅H₄₂N₃O₈SNa), [M-Na]⁻, calculated *m/z*: 544.3, observed *m/z*: 544.2.

Synthesis of the Azobenzene (AZO) surfactant family.

The AZO surfactant family was synthesized following similar procedures as previously described²⁴ (Supplementary Note 3). Specifically, 4 mmol of 4-n-hexylaniline (**n= 4, C6**) was stirred in a mixture of 4.8 mL of 10% hydrochloric acid and 8 mL of DI H₂O. Then 4 mmol of NaNO₂ dissolved in 4 mL of cold water, was added dropwise to this solution. During the addition of the NaNO₂ the solution was cooled to 10 °C. After the addition was completed (15 min), the solution was stirred for an additional 15 min at 5 °C. A similar procedure was carried out for 4-n-octylaniline (**n=6, C8**). For 4-n-decylaniline (**n= 8, C10**) and 4-n-dodecylaniline (**n= 10, C10**), the solution of 4-n-alkylaniline was heated to 70 °C and then cooled in an ice bath to 10 °C under vigorous stirring. NaNO₂ was added dropwise

starting at 20 °C and concluded at 10 °C, followed by 15 min of stirring at 5 °C. For the coupling reaction, the freshly prepared diazonium salt was filtered into a stirring and cooled solution (T= 5–10 °C) of 8 mmol of Na₂SO₃ and 12 mmol of Na₂CO₃ in 20 mL of DI H₂O. To complete the precipitation of the surfactant, the solution was refrigerated at 4 °C overnight. The yellow compounds were purified by recrystallization with a yield about 50% and no impurities were detected by NMR. Surfactant solutions were made by gently heating the surfactant at 37 °C then bringing to room temperature after no solid remained. Working concentration was 0.5%–1% in 25 mM NH₄HCO₃. Kraft temperature (a clear 1% surfactant solution) was previously reported at 24.5 °C⁷. A high-resolution mass spectrum of AZO (C6), referred to as Azo, (Supplementary Figure 1) was taken as follows: A solution of 1% Azo in 25 mM NH₄HCO₃ was diluted 1:100 in ACN (0.3% NH₄OH). The sample was directly injected into a 7 T linear ion trap/Fourier transform ion cyclotron resonance (LTQ/FT-ICR) mass spectrometer (LTQ/FT Ultra, Thermo Scientific, Bremen, Germany) with a nano-ESI source (Triversa NanoMate; Advion Bioscience, Ithaca, NY). A voltage of –1.4 kV was applied with 0.3 psi drying gas. 50 scans were averaged with 5 microscans in a scan. The mass range was set from 100 to 500 *m/z*. ESI-MS for Azo (C₁₂H₁₇N₂O₃SNa), [M-Na][–], calculated *m/z*: 269.096, observed *m/z*: 269.098. A Hermes-Varian Mercury Plus 300 operating at 300 MHz was utilized for ¹H-NMR spectroscopy with chemical shifts reported as ppm (parts per million). ¹H NMR: δ 7.64 (2H, dd, -Ar-H), 7.37 (2H, d, -Ar-H), 2.67–2.48 (2H, m, -Ar-CH₂), 1.61 (2H, t, -Ar-CH₂CH₂), 1.28 (6H, t, -(CH₂)₃) .086 (3H, t, -(CH₂)₃-CH₃).

Tissue handling.

Swine hearts were excised from healthy Yorkshire domestic pigs, snap-frozen in liquid N₂, and stored under –80 °C before use. All homogenization and centrifugation steps were performed at 4 °C.

Protein extraction and LC-MS analysis of cardiac tissue.

The frozen tissue samples (~500 mg) were cut into small pieces and washed with PBS buffer containing protease inhibitors and reducing agent (5 mM DTT, 1 mM PMSF, 1x protease inhibitor cocktail). The tissue was then homogenized in HEPES buffer with both protease and phosphatase inhibitors (25 mM HEPES, 250 mM sucrose, 50 mM NaF, 1 mM PMSF, 2.5 mM EDTA, 1 mM Na₃VO₄, 1 mM PMSF, 5 mM DTT, 1x protease inhibitor cocktail) with a Polytron electric homogenizer (model PRO200, Pro scientific, Oxford, CT) set to the lowest speed as described previously¹⁰. The homogenate was centrifuged at 211,750 × *g* using Beckman Ultracentrifuge and a Ti-80 rotor for 1 h. The supernatant after the first HEPES extraction was removed and saved as “E1” extraction. The HEPES extraction was repeated on the resulting pellet and saved as “E2”. After the second HEPES extraction, the tissue pellet was suspended in 25 mM NH₄HCO₃ and evenly divided into smaller aliquots. In one aliquot, 25 mM NH₄HCO₃ buffer with no surfactant (NS) serving as controls was used in a 1:1 ratio (homogenate:buffer) and labeled as “E3(NS)” following incubation and centrifugation. In the other aliquots, surfactants (1% in 25 mM NH₄HCO₃) were individually added to the other aliquots in a 1:1 ratio (homogenate: surfactant) and labeled as “E3(Surfactant)” following incubation and centrifugation. Protein assays were performed using Pierce 660 nm Protein Assay Reagent with Ionic Detergent Compatibility Reagent

(<https://www.thermofisher.com/order/catalog/product/22660>) for data presented in Figure 1f and BCA protein assay (with 5% SDS compatible) for data presented in Supplementary Figure 10.

Reversed phase chromatography (RPLC) was performed with a nanoACQUITY M-Class UPLC system (Waters; Milford, MA, USA). Mobile phase A (MPA) contained 0.2% formic acid in H₂O, and mobile phase B (MPB) contained 49.9% ACN: 49.9% IPA: 0.2% formic acid. For each injection, 5 µL of sample was loaded on a home-packed [250 × 0.250 mm or 0.5 mm, 5 µm, 1000 Å PLRP-S (Agilent Technology, Santa Clara, CA, USA)]. Samples eluted from the column were electrosprayed into a maXis II ETD Q-TOF mass spectrometer (Bruker Daltonics, Bremen, Germany) for online LC-MS and LC-MS/MS experiments. End plate offset and capillary voltage were set at 500 and 4500 V, respectively. The nebulizer was set to 0.5 bar, and the dry gas flow rate was 4.0 L/min at 220 °C. The quadrupole low mass cutoff was set to 600 *m/z* during MS and 200 *m/z* during MS/MS. Mass range was set to 200–3,000 *m/z* and spectra were acquired at 1 Hz for LC-MS runs. For the top 3 data-dependent LC-MS/MS collision-induced dissociation (CID) runs, MS/MS spectra were acquired across 200–2,500 *m/z* at 2–4 Hz with active exclusion after 4 spectra. Targeted LC-MS/MS CID was performed at 1 Hz after determining the elution time frame from the targeted proteins.

20 µL of cardiac tissue lysate with or without Azo (referred to as “Azo” or “NS”, respectively) was added 116 µL H₂O, 2 µL of HFIP (5%), 2 µL trifluoroacetic acid (10%), 10 µL TCEP (1 M), 50 µL IPA, 50 µL ACN. Reagents were added slowly and mixed throughout to avoid precipitation. The samples were transferred to a quartz cuvette and irradiated for 3 min using a 100 w high pressure mercury lamp. The resulting samples were exchanged into 20% ACN: IPA (1% formic acid) with a 10 kDa MWCO centrifugal filter and adjusted to a final volume of 150 µL. Protein were separated using the following conditions 0–5 min 20% B, 5–25 min 20–60% B, 65–75 min 60–75% B, 75–80 min 75–95% B, 85–86 min 95–20%B, 86–95 min 20% B. The methods described here correspond to the data presented in Figure 3, Supplementary Fig. 13–15, 17–19, and Supplementary Table 2–8.

SDS-PAGE comparing Azo with SDS, DDM, and MaSDeS.

An equal volume (7 µL) of each extraction was subsequently resolved using 12.5% SDS-PAGE with a voltage of 50 V for 30 min and 120 V for approximately 75 min. Proteins were visualized using Coomassie Brilliant Blue R-250. The methods described here correspond to data presented to Figure 1e.

Western blot comparing Azo with SDS, DDM, and MaSDeS.

Equal volumes of tissue lysate (10 µL) were loaded and resolved on 12.5% SDS-PAGE gels. Proteins were transferred to a PVDF membrane, fast semi-dry blotter (Fisher Scientific, Waltham, MA), using 20 V for 12 h at 4 °C. The membrane was placed in a protein-free blocking buffer (Fisher Scientific, Waltham, MA) for 1 h at RT and incubated with primary antibodies for 1.5 h at RT. The membranes were then washed by using TBS with 0.1% tween five times before incubation with the secondary antibodies for 1.5 h (RT). After 5

washes with TBS with 0.1% tween, the membranes were developed using enhanced chemiluminescence detection (Fisher Scientific, Waltham, MA). The methods described here correspond to data presented in Supplementary Figure 5).

Comparison of the top-down MS compatibility of Azo with SDS, DDM, and MaSDeS.

Ubi was dissolved in a buffer containing 80: 5: 5: 10 IPA: H₂O: formic acid: 1% surfactant (Azo, SDS, DDM, or MaSDeS) with 10 mM DTT. The Azo sample was irradiated for 3 min. The MaSDeS sample was degraded for 24 h at RT. The samples were then directly injected into a 7 T linear ion trap/Fourier transform ion cyclotron resonance (LTQ/FTICR) mass spectrometer (LTQ/FT Ultra, Thermo Scientific, Bremen, Germany) with a nano-ESI sprayer (TriVersa NanoMate; Advion Bioscience, Ithaca, NY). A voltage of 1.4 kV vs the inlet was applied with 0.3 psi drying gas. 50 scans were collected with 5 microscans in one scan. The mass range was set from 600 to 2,000 *m/z*. The methods described here correspond to data presented in Figure 1g.

Protein extraction and LC-MS analysis of sarcoplasmic reticulum (SR) and mitochondria (Mit) enrichment from cardiac tissue.

After cutting around 170 mg of tissue into small pieces, the tissue was homogenized in HEPES buffer containing both protease and phosphatase inhibitors (50 mM HEPES, 0.6 M KCl, 250 mM Sucrose, 500 mM NaF, 1 mM PMSF, 2 mM EDTA, 1 mM Na₃VO₄, 5 mM DTT, 25 µg/mL DGT, 1x protease inhibitor cocktail) with a Polytron electric homogenizer set to the lowest speed (tissue) to deplete soluble proteins as described previously²⁵. The homogenate was centrifuged at 20,000 × *g* using a Thermo Scientific Legend Micro 21R Ultracentrifuge. The supernatant was removed and labeled as “E1”. The pellet was suspended in the buffer (25 mM NH₄HCO₃, 500 mM NaF, 1 mM PMSF, 2 mM EDTA, 1 mM Na₃VO₃, 5 mM DTT, 25 µg/mL digitonin, 1x protease inhibitor cocktail) to remove residual proteins and labeled as “E2”. The resulting tissue pellet was suspended in 25 mM NH₄HCO₃ and evenly divided into smaller aliquots, centrifuged at 20,000 × *g*, and the supernatant was removed. 25 mM NH₄HCO₃ buffer (NS) or 1% Azo in 25 mM NH₄HCO₃ was added to the aliquots respectively. After homogenization and incubation, the samples were centrifuged and the supernatant was collected.

50 µL of enriched sarcoplasmic reticulum and mitochondria lysate from cardiac tissue was diluted with 440 µL of 50: 48.5: 1: 0.5 IPA: H₂O: formic acid: HFIP and 10 µL of TCEP (1 M). The sample was irradiated for 3 min and concentrated to a final volume of 150 µL MWCO (10 kDa in run 1 or 30 kDa in run 2). Proteins were separated using the following gradient: 0–1 min 5% B, 1–5 min 5–30% B, 5–55 min 30–60% B, 55–57 min 60–95% B, 57–65 min 95%B, 65–67 min 95% B, 67–80 min 5% B. Column temperature was 35 °C. For ATP synthase subunit α, a single charge state was isolated and fragmented with 5, 10, 16, 18, 20 eV, respectively, using an isolation window of 3 *m/z* during targeted CID MS/MS experiments. The methods described here correspond to data presented in Figure 3, Supplementary Fig. 13–15, 17–19, and Supplementary Table 2–8).

Protein extraction and LC-MS analysis of endoplasmic reticulum (ER) and mitochondria (Mit) enriched lysate from human embryonic kidney (HEK) 293T cells.

Cells were grown on 10 cm plates in DMEM with 10% fetal bovine serum and 1x penicillin/streptomycin solution at 37 °C and 5% CO₂. Cells from two 10 cm plates were washed twice with PBS and lysed in 500 µL of buffer (10 mM Tris, 2 mM DTT, 1 mM PMSF, 50 µg/mL DGT, 1x protease inhibitor cocktail) using 50 strokes with dounce homogenizer followed by 5 passages through a 27 G needle. Cells were then incubated for 10 min on ice, evenly divided into two aliquots, and centrifuged at 1,000 × g (4 °C) to remove unbroken cells and the nuclei. The supernatant was mixed with 0.5 mL of sucrose (50%) and centrifuged at 21,000 × g (4 °C). The pellet was washed with 1 mL of NH₄HCO₃ (E2). Finally, the pellets were dissolved in 100 µL of Azo (0.5% in 25 mM NH₄HCO₃) or 100 µL of 25 mM NH₄HCO₃ without surfactant (NS) serving as controls.

50 µL of enriched endoplasmic reticulum and mitochondria lysate from HEK cells was diluted with 400 µL of 50% IPA: 49% H₂O: 1% formic acid and 50 µL of TCEP (1M). The sample was irradiated for 3 min then concentrated and exchanged into 10:10:80 ACN: IPA: 1% formic acid in H₂O with a 10 kDa MWCO centrifugal filter. Protein were separated using the following gradient: 0–5 min 20% B, 5–65 min 20–95% B, 65–75 min 95% B, 75–76 min 20% B, 76–80 min 20% B. Column temperature was 50 °C. The methods described here correspond to data presented in Supplementary Fig. 16 and Supplementary Table 9–10.

Azo-PAGE and SDS-PAGE comparison.

Resolving gel was made using 1.62 mL water, 2.09 mL acrylamide, 1.25 mL Tris-base (1.5 M, pH 8.8), 0.05 APS (10%), and 0.002 mL TEMED. Stacking layer was made using 1.42 mL water, 0.33 mL acrylamide, Tris-base (1 M, pH 6.8), 0.02 APS (10%), and 0.002 mL TEMED. 2.5 µg of BSA, β-casein, and RNase A or 10 µg of cardiac myofibrillar extract²⁶ was separated on a 1 mm, 12.5% polyacrylamide gel running at 150V. Azo Loading Dye (2x) consisted of 100 µL Tris (1M pH 6.8), 10 mg Azo, 200 µL bromophenol blue (0.04% solution), 200 µL glycerol, 20 µL DTT (1M), and adjusted the volume to 1 mL with water. Azo running buffer was made using 1.5 g Tris base, 7.2 g Glycine, 2.5 g Azo, and adjusted the volume to 1 L with water. The SDS-PAGE comparison gel was run using the same condition except 20 mg of SDS was used in the Loading Dye and 0.5 g of SDS was used in the running buffer. The methods described here correspond to data presented in Supplementary Figure 3.

UV-Vis degradation.

50 µL of 0.1% Azo in (a) H₂O, (b) 1% formic acid, (c) IPA, (d) 1% formic acid in IPA, (e) 2-ME in H₂O, and (f) 1% formic acid in IPA: H₂O, respectively, were irradiated with 100 W high pressure mercury lamp (Nikon housing with Nikon HB-10101AF power supply; Nikon, Tokyo, Japan) for 0, 10, 30, 60, 90, and 120 s in a quartz cuvette. The samples were diluted to a final volume of 1 mL in H₂O. A UV-Vis spectrum was taken from each sample with a Varian Cary 50 UV-Visible spectrophotometer (background correction, medium scan rate, 600–200 nm). The methods described here correspond to the data presented in Supplementary Figure 4.

Evaluation of the effect of reducing agents during Azo degradation.

Standard proteins, Ubi, RNase A, Cyt c , and BSA were dissolved in 49.5:49.5:1 H $_2$ O: IPA: formic acid and kept on ice until analysis. Samples were irradiated with a 100 W lamp for 3 min. 5 μ L of sample was injected onto a trap column and eluted with 40:40:20 ACN: IPA: 1% formic acid in H $_2$ O after a 5 min wash with 2.5:2.5:95 ACN: IPA: 1% formic acid in H $_2$ O. 50 mM of DTT, TCEP, and 2-ME were added to each Cyt c samples prior to irradiation. Additionally, a sample of Cyt c was kept at RT with no reducing agent and irradiated for 3 min with no reducing agent as a control (corresponding to Supplementary Figure 6–7). This method was repeated to test 10 mM TCEP and 33 mM methionine (corresponding to Supplementary Figure 8).

Protein extraction and LC-MS analysis for evaluating the effect of Azo on relative quantitation.

10 volumes of buffer (10 mM Tris, 500 mM NaF, 2 mM EDTA, 1 mM PMSF, 1 mM Na $_3$ VO $_4$, 5 mM DTT) was added to swine heart tissue. The sample was homogenized with Teflon homogenizer, centrifuged at 16,000 \times g, and the supernatant was collected. Protein extract was diluted to a final buffer containing 25% IPA, 25% ACN, 1% formic acid, 100mM TCEP, and 5 mM NH $_4$ HCO $_3$ with or without 0.2% Azo. The sample was irradiated for 3 min and exchanged into a 10% ACN, 10% IPA, with 0.2% formic acid using a 10 kDa MWCO centrifugal filter. Protein were separated using the following gradient: 0–5 min 20% B, 5–30 min 20–65% B, 30–35 min 65% B, 35–36 min 20% B, 36–40 min 20% B. Column temperature was 60 $^{\circ}$ C. The methods described here correspond to the data presented in Supplementary Figure 9.

Comparison of the top-down MS compatibility of Azo to a broader range of commonly used surfactants.

Ubi was dissolved in buffer containing 75: 10: 5: 10 MeOH: H $_2$ O: formic acid: 1% surfactant (MaSDeS, PM, RG, NS, SDS, Azo, OG, DDM, DGT) with 10 mM TCEP. The Azo sample was irradiated for 3 min. The acid-labile surfactants were incubated for 75 min (24 h for MaSDeS) at 37 $^{\circ}$ C. The samples were then directly injected into a 12 T Fourier transform ion cyclotron resonance (solariX) mass spectrometer (Bruker Daltonics, Bremen, Germany) with a nano-ESI sprayer (TriVersa NanoMate; Advion Bioscience, Ithaca, NY). A voltage of 1.4 kV vs the inlet was applied with 0.3 psi drying gas. 200 scans were averaged for each sample. The mass range was set from 600 to 2,000 m/z with a 512,000 word transient. The methods described here correspond to the data presented in Supplementary Figure 11.

Protein extraction for top-down LC-MS compatibility comparing Azo to MaSDeS, PM, RG, SDS, OG, DDM, DGT.

83.3 mg of swine cardiac tissue was homogenized in 1 mL of buffer (25 mM NH $_4$ HCO $_3$, 1 mM TCEP, and 1 mM PMSF). After centrifugation at 16,000 \times g, the supernatant was collected and the protein concentration was adjusted to 2 mg/mL. To 15 μ L of swine cardiac protein extract (2 mg/mL) was added 1.5 μ L water, 6 μ L methionine (25 mg/mL), 25 μ L isopropanol, 5 μ L TCEP (100 mM), and 2.5 μ L formic acid. The Azo sample was irradiated

for 3 min. The acid cleavable surfactants PM²¹ and RG¹¹ (also known as ALS¹³) were incubated at 37 °C for 1 h while MaSDeS was incubated at 37 °C for 24 h due to its slow degradation¹⁰. All samples without (NS) or with the surfactants (MaSDeS, PM, RG, SDS, Azo, OG, DDM, DGT) were buffer exchanged into 10 % ACN, 10 % IPA, and 1 % FA using a MWCO filter (3 × 100 µL) and adjusted to the original volume of 50 µL. Protein were separated using the following gradient: 0–5 min 20% B, 5–30 min 20–65% B, 30–35 min 65% B, 35–36 min 20% B, 36–40 min 20% B. Column temperature was 60 °C. Column temperature was 60 °C. The methods described here correspond to the data presented in Supplementary Figure 12.

Data Analysis.

Data were analyzed and processed in DataAnalysis 4.3 (Bruker Daltonics). An msalign file was created using SNAP peak picking algorithm with the following parameters: quality factor (0.4); S/N (3); intensity threshold (500); retention window (1.5 min). The file contained the following information: precursor mass, precursor charge, precursor mass followed by the fragment masses, intensities, and charges. TopPIC²⁷ was utilized for intact protein identification based on protein spectrum matches searching against the UniProt *Sus scrofa* (released on Nov. 22nd, 2017; containing 26817 protein sequences) or *Homo sapiens* (released on Dec. 20th, 2017; containing 20244 reviewed protein sequences) database²⁸. Fragment mass tolerance was set to 15 ppm. All identifications were validated with statistically significant P and E values (<E-5) and satisfactory numbers of assigned fragment ions (>6). Sequence mass determination and validation was performed using Mash Suit Pro²⁹ or ProSight Lite³⁰. The corresponding MS and MS/MS data were summarized in Supplementary Table S4–10. UniProt gene ontology³¹ was used to determine the subcellular location of the identified proteins which were then graphed in Excel. String analysis software³² was used to create an interactome map of identified proteins belonging to the electron transport chain.

The proteoform maps were generated as follows: (1) LC-MS scans were averaged every min; (2) deconvoluted using Maximum Entropy algorithm (Resolution: 80,000; mass range: 5,000–60,000 Da); (3) mass list outputs were generated using SNAP peak picking (quality factor: 0.8, S/N: 3, absolute intensity 1,000) as described previously³³. A graphic map was then generated in Microsoft Excel based on the first retention time and the monoisotopic mass generated from SNAP. The methods described here correspond to the data presented in Supplementary Figure 13.

Statistical analysis.

For the protein solubility experiment (Figure 1f) comparing Azo, SDS, DDM, and MaSDeS, three independent protein assays (n=3) were performed to evaluate surfactant performance. Error bars represent standard error of the mean. For the broader protein solubility comparison (Supplementary Fig. 10), data presented were based on three independent experiments (n=3). Error bars represent standard error of the mean. For LC-MS analysis (Supplementary Fig. 9), three separate samples (n=3) were prepared for each condition. Error bars represent standard error of the mean.

Reporting Summary.

Nature Life Science Reporting Summary is linked to this article for further information regarding the research design.

Data Availability

All data generated or analyzed during this study is presented in this manuscript or in the provided. Moreover, proteomics data has been uploaded to PRIDE repository via ProteomeXchange with identifier PXD010825.

Supplementary Material

Refer to Web version on PubMed Central for supplementary material.

Acknowledgement

This research is supported by NIH R01 GM117058 (to S.J. and Y.G.). Y. G. would like to acknowledge R01 HL109810, R01 HL096971, R01 GM125085, and S10 OD018475 (to Y.G.). We thank A. Chen, E. Chang and W. Tang for their assistance in the early stage of the project, S. Mitchell and T. Tucholski for the help with graphics, and T. Hacker for providing the swine hearts. We would like to thank Matt Willetts at Bruker for his assistance with DataAnalysis software. We would also like to acknowledge A. Carr, E. Bayne, and J. Melby for their help testing the Supplementary Protocol to ensure reproducible results.

REFERENCES

1. Aebersold R et al. *Nat. Chem. Biol* 14, 206 (2018). [PubMed: 29443976]
2. Siuti N & Kelleher NL *Nat. Methods* 4, 817–821 (2007). [PubMed: 17901871]
3. Cai WX, Tucholski TM, Gregorich ZR & Ge Y *Expert Rev Proteomics* 13, 717–730 (2016). [PubMed: 27448560]
4. Chen B, Brown KA, Lin Z & Ge Y *Anal. Chem* 90, 110–127 (2018). [PubMed: 29161012]
5. Barrera NP & Robinson CV *Annu. Rev. Biochem* 80, 247–271 (2011). [PubMed: 21548785]
6. Speers AE & Wu CC *Chem. Rev* 107, 3687–3714 (2007). [PubMed: 17683161]
7. Loo RR, Dales N & Andrews PC *Protein Sci* 3, 1975–1983 (1994). [PubMed: 7703844]
8. Wisniewski JR, Zougman A, Nagaraj N & Mann M *Nat. Methods* 6, 359–362 (2009). [PubMed: 19377485]
9. Kachuk C & Doucette AA *J. Proteomics* 175, 75–86 (2018). [PubMed: 28286130]
10. Chang Y-H et al. *J. Proteome Res* 14, 1587–1599 (2015). [PubMed: 25589168]
11. Yu YQ, Gilar M, Lee PJ, Bouvier ES & Gebler JC *Anal. Chem* 75, 6023–6028 (2003). [PubMed: 14588046]
12. Chen EI, Cociorva D, Norris JL & Yates JR J. *Proteome Res* 6, 2529–2538 (2007). [PubMed: 17530876]
13. Meng F et al. *Anal. Chem* 74, 2923–2929 (2002). [PubMed: 12141648]
14. Bradley M, Vincent B, Warren N, Eastoe J & Vesperinas A *Langmuir* 22, 101–105 (2006). [PubMed: 16378407]
15. Hwang L, Guardado-Alvarez TM, Ayaz-Gunner S, Ge Y & Jin S *Langmuir* 32, 3963–3969 (2016). [PubMed: 27046005]
16. Kim MS & Diamond SL *Bioorg. Med. Chem. Lett* 16, 4007–4010 (2006). [PubMed: 16713258]
17. Dunkin IR, Gittinger A, Sherrington DC & Whittaker PJ *Chem. Soc., Perkin Trans. 2* 1837–1842 (1996).
18. Laganowsky A, Reading E, Hopper JTS & Robinson CV *Nat. Protoc* 8, 639–651 (2013). [PubMed: 23471109]
19. MacLennan DH & Kranias EG *Nat. Rev. Mol. Cell Biol* 4, 566–577 (2003). [PubMed: 12838339]

20. He J et al. *Proc. Natl. Acad. Sci* (2018).
21. Saveliev SV et al. *Anal. Chem* 85, 907–914 (2013). [PubMed: 23256507]
22. Lee HB et al. *J. Org. Chem* 69, 701–713 (2004). [PubMed: 14750794]
23. Posselius JHF et al. United States Patent Application Publication. *Biological Systems Engineering: Papers and Publications*. 468 (2014).
24. Mezger T, Nuyken O, Meindl K & Wokaun A *Prog. Org. Coat* 29, 147–157 (1996).
25. Wientzek M & Katz SJ *Mol. Cell. Cardiol* 23, 1149–1163 (1991).
26. Peng Y et al. *Mol. Cell. Proteomics* 13, 2752–2764 (2014). [PubMed: 24969035]
27. Kou Q, Xun L & Liu X *Bioinformatics* 32, 3495–3497 (2016). [PubMed: 27423895]
28. Apweiler R et al. *Nucleic Acids Res* 32, D115–119 (2004). [PubMed: 14681372]
29. Cai W et al. *Mol. Cell. Proteomics* 15, 703–714 (2016). [PubMed: 26598644]
30. Fellers RT et al. *Proteomics* 15, 1235–1238 (2015). [PubMed: 25828799]
31. Ashburner M et al. *Nature Genet.* 25, 25–29 (2000). [PubMed: 10802651]
32. Szklarczyk D et al. *Nucleic Acids Res.* 45, D362–D368 (2017). [PubMed: 27924014]
33. Cai W et al. *Anal. Chem* 89, 5467–5475 (2017). [PubMed: 28406609]

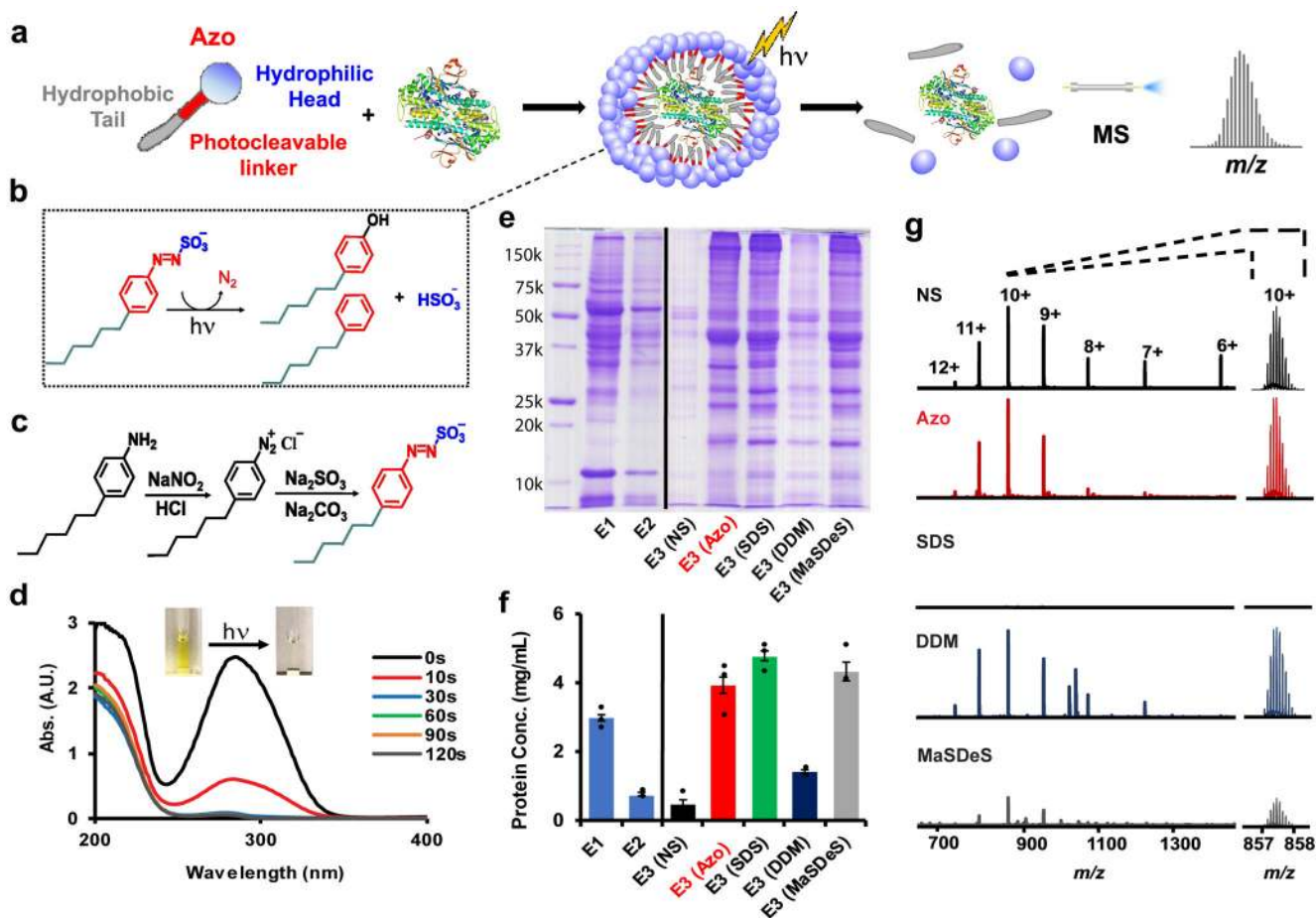


Figure 1 | Synthesis and characterization of a photo-cleavable anionic surfactant, sodium 4-hexylphenylazosulfonate (Azo).

(a) Scheme illustrating the use of Azo in solubilizing proteins, followed by rapid degradation with UV irradiation, and MS analysis of the intact proteins. Note that the molecules are not drawn to scale. (b) Degradation of Azo into 4-hexylphenol, 4-hexylbenzene, nitrogen, and hydrogen sulfate under UV irradiation. (c) Synthetic scheme for Azo. (d) UV-Vis spectra of Azo (0.1%) degradation as a function of time showing that Azo can be rapidly degraded upon UV irradiation at ambient temperature. (e) SDS-PAGE analysis and (f) protein assay for the evaluation of effectiveness of surfactant aided protein extractions (E3) following the initial HEPES buffer extractions (E1 & E2) to deplete the cytosolic proteins. Error bars represent standard error of the mean for protein assay experiments ($n=3$). (g) Electrospray ionization (ESI)-MS analysis of Ubi with 0.1% surfactant showed the MS-compatibility of surfactants. The mass spectra were normalized to an intensity of $1.7E6$. NS, no surfactant (serving as a control); Azo; SDS, sodium dodecyl sulfate; DDM, n-dodecyl β -D-maltoside; MaSDeS, MS-compatible slowly degradable surfactant. Data are representative of three independent experiments.

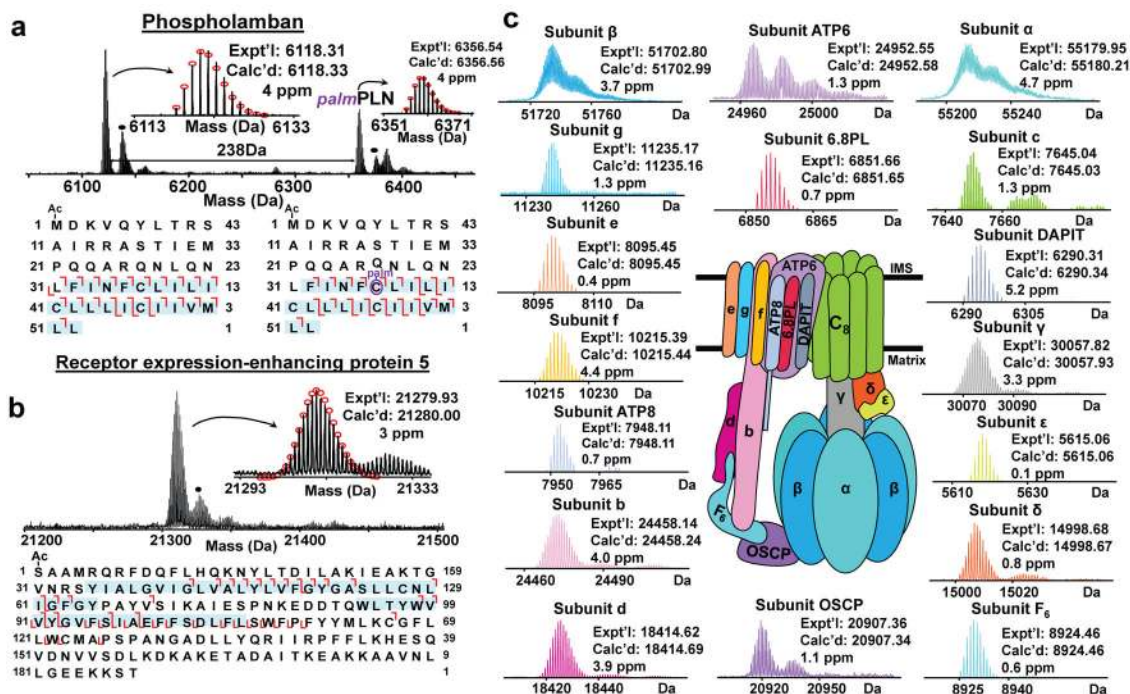


Figure 2 | Photo-cleavable Azo-enabled top-down membrane proteomics.

MS and MS/MS analysis of representative membrane proteins from Azo-aided extraction of cardiac tissue: (a) phospholamban (PLN) and palmitoylated-phospholamban with palmitoylation identified at cysteine 37 residue, (b) receptor expression-enhancing protein 5, and (c) complete analysis of ATP synthase subunit proteins from cardiac tissue. Overall all ATP synthase subunits (e, f, g, ATP6, ATP8, DAPIT, C₆, 6.8PL) that exist in the inner membrane space (IMS) as well as the subunits (α , β , b, e, δ , OSCP, F₆, d, γ) located in the mitochondrial matrix were detected. The schematic of ATP synthase was modified based on a previous publication by He et al²⁰. Data are representative of two independent experiments.